Al-Furat Journal of Innovations in Electronics and Computer Engineering (FJIECE)
ISSN -2708-3985

Comparison Between Hysteresis and Carrier SPWM Current Control Methods of Grid Tied PV Inverter

Nasir Hussein Selman [1], Jawad Radhi Mahmood [2]

[1] *Department of Communications Technical Engineering, Al-Najaf Technical Engineering College/ Najaf, Al-Furat Al-Awsat Technical University ATU, Najaf, 54001, Republic of Iraq, coj.nas@atu.edu.iq*

[2] *Electrical Engineering Department, College of Engineering Basrah University Basrah, Iraq, alali.jhana@yahoo.com*

[*]Corresponding author E-mail: coj.nas@atu.edu.iq

https://doi.org/10.46649/fjiece.v3.1.1a.10.4.2024

Abstract. *This paper has been studying two current control techniques for the two stages single-phase grid-tied photovoltaic (PV) inverter. These control techniques are Sinusoidal pulse width modulation (SPWM) and Hysteresis current. The whole structure of the grid-tied PV inverter has been studied in details for each of its parts. For comparison between the two techniques, the designed system has been tested under MATLAB/Simulink environment for different cases such as insolation and load variation. Results found that the Hysteresis current control method has a simple structure where it does not need PWM block, but it produces a higher total harmonic distortion (THD) as compared with the SPWM method*

Keywords: *PV system, DC-DC boosts converter, MPPT algorithm, LCL filter, current control methods, grid tied inverter.*

1. INTRODUCTION

The world trend in the last years to employ the distributed generators systems with the main electric grid at the distribution levels in order to boost the reliability and stability, decrease power losses, and regulate the voltage of the electrical grid [1]. The PV generator system is an essential part of the distributed generators for being environmentally friendly, renewable, and a considerable reduction in the cost of the PV modules nowadays. Besides that, PV modules don't contain rotating parts, thus a long lifetime was ensured with easy maintenance [2].

A power inverter is required to convert the DC power from the PV arrays. It can be operated as a standalone mode to feed the local AC load or as a grid-tied mode to transfer the extra power to the grid after ensuring a certain grid interconnection requirement standards [3].

Grid-tied inverters can be controlled by many techniques such as Hysteresis current controller (HCC), sinusoidal pulse width modulation (SPWM) control, PI controller, H-infinity controller, proportional resonant controller, repetitive controller, dead beat controllers, ... etc [4]. The most commonly used techniques for control of grid-tied inverter are SPWM control and HCC. Both techniques have advantages and drawbacks [5].

Many studies have been published on grid-tied inverter using different control techniques. P. Rajesh et al [4] have presented a modification of a PI controller for the grid-tied inverter to reduce the steady-state errors in the sinusoidal signal. The simulation results give that the quality of the tracking signal and THD

ATU-FJIECE, Volume: 3, Issue: 01, Apr, 10, 2024, © 2020 FJIECE, All Rights Reserved

Al-Furat Journal of Innovations in Electronics and Computer Engineering (FJIECE)
ISSN -2708-3985

with the modified PI controller is better than the traditional PI controller. M. Antchev and A. T. Mitovska [5] have introduced a study to compare two control methods for grid-connected inverter, HCC and a combination of fuzzy logic (FL) with HCC. The Hysteresis band in the classical HCC method is constant whereas in the case of the combined FL with HCC method has various values that depend on the difference between reference current and the inverter output current. The study shows that both methods are given good efficiency, but the combined method gives fewer harmonics content. H. Su Bae et al [6] have suggested a new method for controlling the two-stage grid-connected solar inverter. The method performs the maximum power point tracking (MPPT) control by measure the inverter's current instead of measure the power of the solar panels. Therefore, the system became simpler and with less cost. D. H. Al Maamoury et al [7] given a MATLAB model system to control the real power of a single-phase grid-connected solar inverter. FL Controller was used to controlling the real power flow for grid-connected mode and Island mode. P. K. Hota1 et al [8] introduced a current control with the PWM method of three-phase grid-tied PV inverter. The PI controller is achieved in the synchronous d-q rotating frame to obtain peak output power. The system was simulated and analyzed by MATLAB SIMULINK for different states. S. D. Patil et al [9] proposed a multilevel inverter for single-phase grid-tied inverter. The control algorithm is based on selective harmonic elimination PWM technique to minimize the harmonics of the inverter current added to the electric network. The control signals are estimated by the Newton Raphson method. A. Chatterjee et al [10] have designed and implemented a digital predictive current control method in the grid-tied inverter. The authors have compared their controller with the proportional resonant current control algorithm. The simulation and practical results confirm the effectiveness of the proposed controller in providing a high power factor and less harmonic value.

In this paper, A 2 kW two-stage single-phase grid-tied PV inverter was covered in detail. The system is controlled by two current control techniques, SPWM and HCC techniques, and compared them in different cases.

The paper is organized as follows: Schematic diagram of the grid-tied PV inverter and its control is studied in Section II. Section III covered simulation results. The conclusion is given in section IV.

II. SCHEMATIC DIAGRAM OF THE PROPOSED GRID-TIED PV INVERTER

The complete block diagram of the proposed grid-tied PV model is depicted in Fig. 1. It consists of the following main stages:.

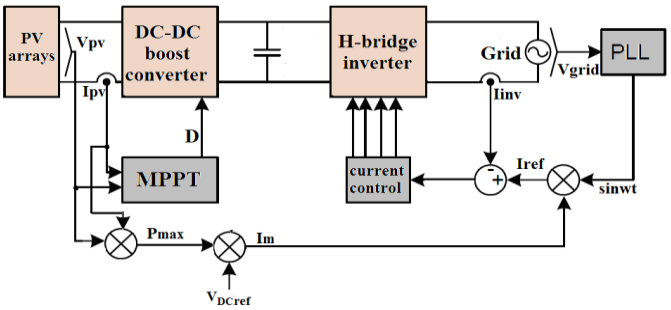

Fig.1. Block diagram of the proposed grid-tied PV inverter

ATU-FJIECE, Volume: 3, Issue: 01, Apr, 10, 2024, © 2020 FJIECE, All Rights Reserved

Al-Furat Journal of Innovations in Electronics and Computer Engineering (FJIECE)
ISSN -2708-3985

A. *PV Arrays System*

The PV arrays framework designed here is consisting of eight SOLIMPEKS type solar panels that are connected in series. The features of the SOLIMPEKS solar panel at Standard Test Conditions (STC) are shown in Table I. The specifications of the whole PV system that was designed are also listed.

Table-I SOLIMPEKS PV panel and whole PV system specifications at STC

Parameters	Specification of PV panel	specifications of the whole PV system
Maximum power	P_m = 240 W	$P_{m\text{-}s}$ =240 x 8 = 1920W
Voltage at maximum power	V_m = 30.72V	$V_{m\text{-}s}$ = 30.72 x8= 245.76V
Current at maximum power	I_m = 7.81 A	I_{ms}= 7.81 A
Open circuit voltage	V_{oc} = 36.6 V	$V_{oc\text{-}s}$ = 36.6x 8 = 292.8 V
Short circuit current	I_{sc} = 8.36 A	$I_{sc\text{-}s}$ = 8.36 A
No. of cells in the panel	60 cells	----
Current Temp. coefficient	$0.4*10^{-3}A/C^0$	---

B. *DC-DC Boost Converter*

DC to DC boost converter is used for extracting the maximum power from the solar panels system. The components of the boost converter have been selected to meet the design specifications tabulated in Table II. Table III offered the parameters and components of the boost converter based on the considerations given in Table II.

Table-II Specifications of the boost converter system

Power rating (P_{max})	≈ 2 kW
Input voltage range (V_{in})	(180 – 250) V
DC Output voltage (V_{out})	≥1.1 $V_{grid\text{-}peak}$
Max. DC load current =P_{max} /V_{out}	≈ 9 A
Switching frequency	10 kHz
V_{out} ripple (ΔV_{out})	≤ 0.5%
I_{in} ripple (ΔI_{in})	≤ 20%

Table-III Boost converter calculated parameters and selected components.

Component	Value/ or Component specifications
MOSFET switch	40A,600V
Diode	40A,600V, Fast recovery diode
Critical inductance value ($L_{crit} = \frac{V_{in}\times D}{f_{sw}\times \Delta I_L}$)	≈3 mH (recommended ferrite teriod core)
Output capacitor($C = \frac{I_{load}\times D}{f_{sw}\times \Delta V_{out}}$)	≈330 µF, 600 V, Electrolytic Capacitor
Maximum duty cycle ($D_{max} = 1 - \frac{V_{in-min}}{V_{out}}$)	0.48
Minimum duty cycle ($D_{min} = 1 - \frac{V_{in-max}}{V_{out}}$)	0.26

ATU-FJIECE, Volume: 3, Issue: 01, Apr, 10, 2024, © 2020 FJIECE, All Rights Reserved

Al-Furat Journal of Innovations in Electronics and Computer Engineering (FJIECE)
ISSN -2708-3985

C. H-bridge Inverter

The H-bridge inverter has been designed according to the specifications given in Table IV. The selection of its components (DC link capacitor and the MOSFETs switches) must meet these specifications. The capacitor is normally added to the output of the boost converter. The MOSFETs must be rated to block the maximum DC bus voltage and carry the maximum expected load current. In practical, the MOSFET voltage ratings are taken to be at least 50% margin over the DC bus voltage. Also the switches must be rated to withstand at least 1.5 times the maximum load current.

Table-IV Specifications of the H-bridge inverter

Power rating (P_{max})	≈ 2 kW
Input voltage (output voltage of the boost converter)	≥ 1.1 $V_{grid\text{-}peak}$
Peak inverter current ≈P_{max}/ 1.1 $V_{grid\text{-}rms}$	≈ 12A
Frequency of AC output	50 Hz ± 1%
Total Harmonics Distortion (THD)	≥ 5%
Switching frequency	10 kHz.

D. L-C-L Filter

In order to supply a pure sinusoidal waveform at the output of the inverter, an LCL filter with damping resistance that is given in Fig. 2 is used. The components of the filter have been discussed and analysis with their equations in references [11]. The same approximation will be applied here to calculate the inverter side inductance (L_{inv}), grid side inductance (L_g), filter capacitance (C_f) and the damping resistance (R_d) and summarized in Table V.

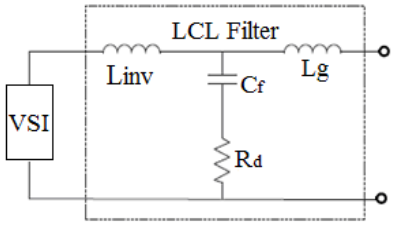

Fig. 2. LCL filter and components

Table-V LCL filter components

Component	Value
Inverter Side Inductor (L_{inv})	1.65 mH
Grid Side Inductor (L_g)	1 mH
Filter Capacitor (C_f)	6 µF
Damping Resistance (R_d)	5 Ω

E. MPPT Controller

Many MPPT methods have been studied in the literature to increase the efficiency of the PV system. The most common methods used have been discussed in reference [12]. Here, the P&O method was used since its simple, low computational effort, and needs only measuring the solar panel voltage and current. In this

ATU-FJIECE, Volume: 3, Issue: 01, Apr, 10, 2024, © 2020 FJIECE, All Rights Reserved

Al-Furat Journal of Innovations in Electronics and Computer Engineering (FJIECE)
ISSN -2708-3985

method, a small perturb in the voltage of the solar panel (ΔV) is presented and then the change in the solar panel power (ΔP) will be observed. The modifications are done in the same direction until there is no more increment in power [13]. If the ΔP is negative, the operating point will move away from the maximum power point (MPP) and the direction of perturbation must be inverted to return toward the MPP.

F. Current Controler

Current control (CC) method is more popular in grid tied inverter. In this algorithm, the inverter output current must track the grid voltage with lower error as possible [14]. This control method can not be performed if the DC link voltage is less than the peak grid voltage plus the voltage drop across the transistor of the inverter and filters [2]. The most interest DC link voltage is about (1.1× grid voltage peak, *i.e* ≈ 345 V).

A block diagram of the CC method used in this study is depicted in Fig. 3. The system consists of a discrete single phase PLL that is used to find a phase angle of the grid voltage signal. The gain at the input of PLL is used to normalize the grid voltage. The output of PLL is multiplied with current (I_m) (current that is obtained from MPPT algorithm) to generate reference current (I_{ref}). The CC block receives the difference between I_{ref} and inverter output current (I_{inv}). The output of the current controller block is the pulses that are sent to the gate of the inverter MOSFETs. The widths of the output pulses are proportional to the amplitude of the difference signal. The inverter works based on these pulses to make its output current synchronizing with the grid voltage.

Two current control methods will be discussed in the following subsections:

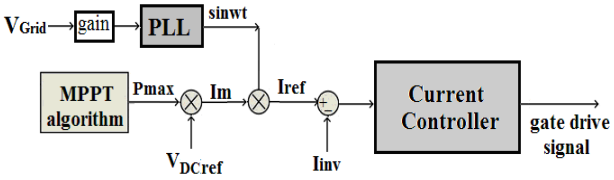

Fig. 3. Current control block diagram

1. SPWM Control Method

The output current of the inverter is controlled with a SPWM control method. A simplified scheme explaining the SPWM control method is shown in Fig.4. The difference between the reference current and the inverter output current is fed to PI controller. Then, the output of the PI controller is compared with sawtooth signal to generate the drive signals to the inverter MOSFETs. The advantage of the SPWM control method is the constant switching frequency. But this method has relatively poor performance when tracking a sinusoidal reference due to the steady-state error.

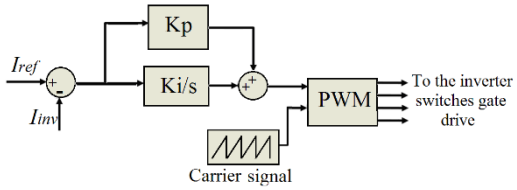

Fig.4. PWM current control method.

2. Hysteresis Control Method

In this method, the switching action of the inverter keeps the current within a certain limit around the sinewave reference current. This limit is called Hysteresis band (*h*) and defined as [15]:

ATU-FJIECE, Volume: 3, Issue: 01, Apr, 10, 2024, © 2020 FJIECE, All Rights Reserved

Al-Furat Journal of Innovations in Electronics and Computer Engineering (FJIECE)
ISSN -2708-3985

$$\left.\begin{aligned} I_{ref-up} &= I_{ref} + \frac{h}{2} \\ I_{ref-down} &= I_{ref} - \frac{h}{2} \end{aligned}\right\} \quad (1)$$

HCC method used here is illustrated in Fig.5. The control system receives two inputs signals, I_{ref} and I_{inv} signals. These currents are subtracted using a difference amplifier with unity gain to generate error signal. HCC compares the error to see signal whether it is in or out of the Hysteresis band.

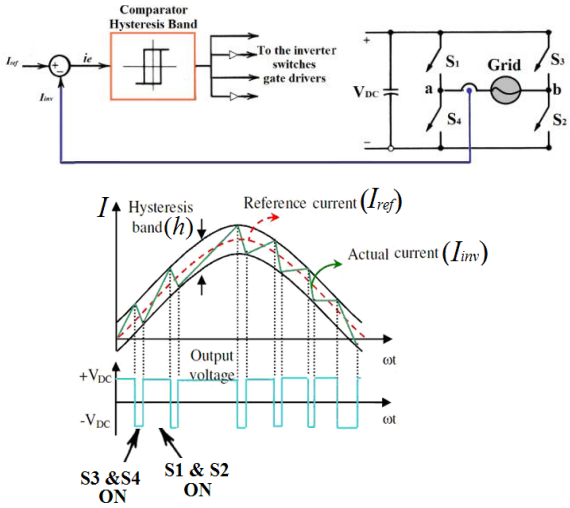

Fig.5. Hysteresis current controller scheme

The output of the Hysteresis controller is the two switching states of the inverter which can be summarized as follows:

- When I_{inv} reaches or exceeds the upper limit of the Hysteresis band (I_{ref-up}), S_1 and S_2 are turned OFF, S_3 and S_4 are turned ON to decreases the current.
- When I_{inv} tries to go below the lower band of Hysteresis ($I_{ref-down}$), the opposite switching occurs and the current increases.

The switching state does not change while the current error remains in the Hysteresis band.

HCC has the advantages of robustness, fast dynamic response and does not need PWM block. But it has a variable switching frequency because it depends on the operating conditions and how fast the current changes from the upper limit to the lower limit and vice versa.

III. Simulation Results and Analysis

To validate the proposed system and to make a comparison between the two CC techniques that have been discussed in this paper, different cases, such as load step changes, insolation variation have been considered.

SPWM Controlled Simulink Model

The Simulink model of the SPWM based control method is given in Fig. 6. The system test is done with the following two cases:

ATU-FJIECE, Volume: 3, Issue: 01, Apr, 10, 2024, © 2020 FJIECE, All Rights Reserved

Al-Furat Journal of Innovations in Electronics and Computer Engineering (FJIECE)
ISSN -2708-3985

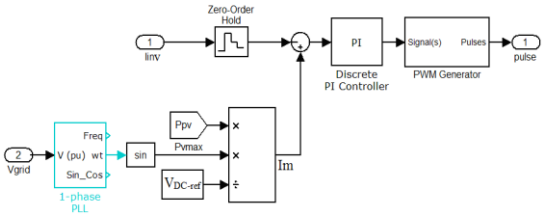

Fig.6. Simulink model of carrier based current control method.

Case 1: Constant PV arrays power with variable load: The system was tested with a resistive load power increased in steps (from no load to 3000 W, and an increase of 750 watts per step). In this case, the PV arrays assumed to generate constant power of 1500W. Figure 7 displays the waveforms of the inverter current (I_{inv}) and the grid voltage (V_{grid}). This figure shows that the inverter output current in phase with the grid voltage.

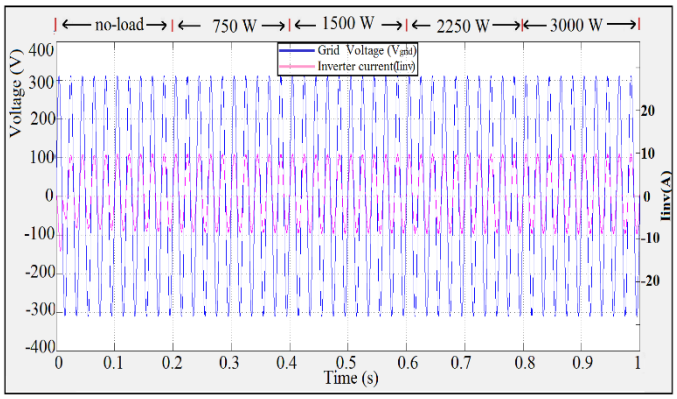

Fig.7. Grid voltage and inverter output current during step load changing and constant PV power.

Figure 8 offers the simulation result of the inverter current (I_{inv}), grid current (I_{grid}) and load current (I_{Load}).

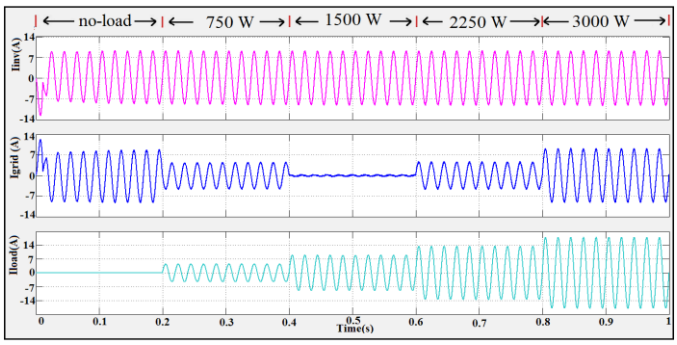

Fig.8. I_{inv}, I_{grid}, and I_{load} during step load changing and constant generated PV power.

From the above figure, the following observations can be noticed:

i- In the absence of load (period from 0 s to 0.2 s), the whole inverter current is injected to the grid. Therefore, the grid current is 180° out of phase with inverter current which refers that the grid is receiving current during this period.

ii- When the inverter power is more than the power required to the loads (period from 0.2 s to 0.4 s), the surplus inverter current is exported to the grid, (i.e. $I_{inv}=I_{Load}+I_{grid}$). In this case, the inverter current and load current are in phase and grid current is 180^0 out of phase. Also, this refers that the grid is receiving the surplus current of the inverter.

ATU-FJIECE, Volume: 3, Issue: 01, Apr, 10, 2024, © 2020 FJIECE, All Rights Reserved

Al-Furat Journal of Innovations in Electronics and Computer Engineering (FJIECE)
ISSN -2708-3985

iii- When a load of (1500 W) is applied (period from 0.4 s to 0.6 s), inverter supplies all current to the load and hence no current transfers to the grid (i.e. $I_{inv} \approx I_{Load}$).

iv- When the load requires current more than the maximum capacity of the PV system (period from 0.6 s to 1 s), the grid contribute part of the required current (i.e. $I_{Load}=I_{inv}+I_{grid}$). In this case inverter, load, and grid currents have the same phase which means that the inverter and grid are supplying current to the load.

Figure 9-a shows that the THD of the inverter current of the SPWM current control method is 1.93%, while Fig. 9-b gives the THD of the current injected to the grid is 2.35% which are both sufficiently satisfy the THD% requirements.

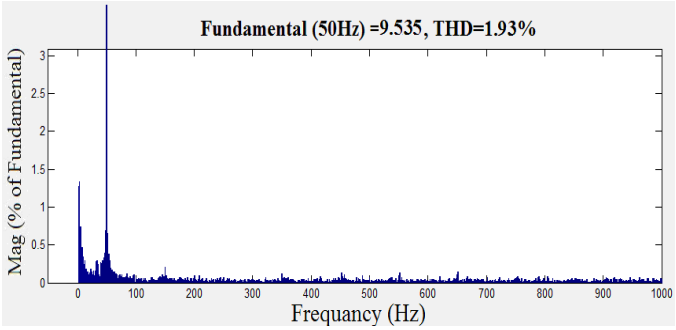

(a) THD and harmonics spectrum of I_{inv}.

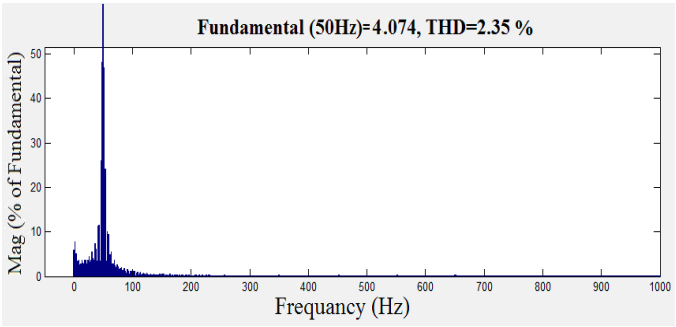

(b) THD and harmonics spectrum I_{Grid}.

Fig. 9. THD and harmonics spectrum of I_{inv} and I_{Grid} during step load changing and constant generated PV power.

***Case 2: Variable PV arrays power with constant inductive load*:** The controller has been tested in presence of power variations which caused by solar insolation variations as given in Fig. 10. The system was examined with inductive load of (1000Watt + 600VAR).

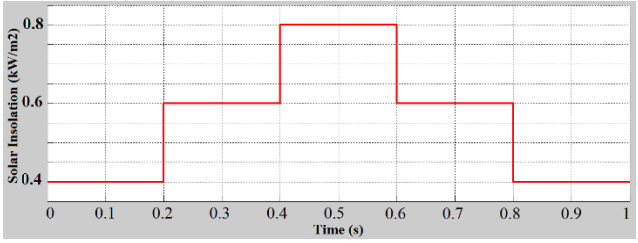

Fig.10. Solar insolation variations (kW/m^2)

The simulation results of the grid voltage and inverter are illustrated in Fig.11. It can be noticed that the inverter current is in phase with grid voltage while its amplitude is proportional to the solar insolation.

ATU-FJIECE, Volume: 3, Issue: 01, Apr, 10, 2024, © 2020 FJIECE, All Rights Reserved

Al-Furat Journal of Innovations in Electronics and Computer Engineering (FJIECE)
ISSN -2708-3985

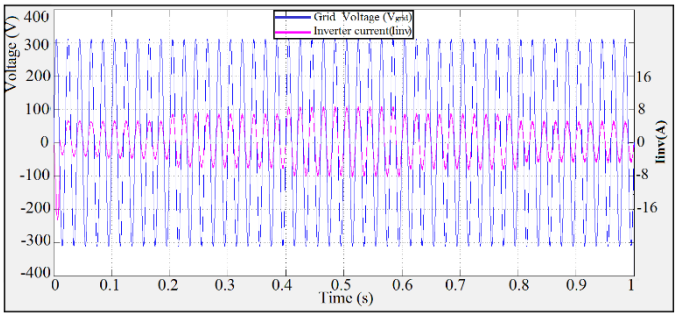

Fig.11: Grid voltage and inverter output current during insolation variations.

The zoomed inverter, grid and load currents are shown in Fig.12 (a, b and c) for three-time intervals with different solar insolation.

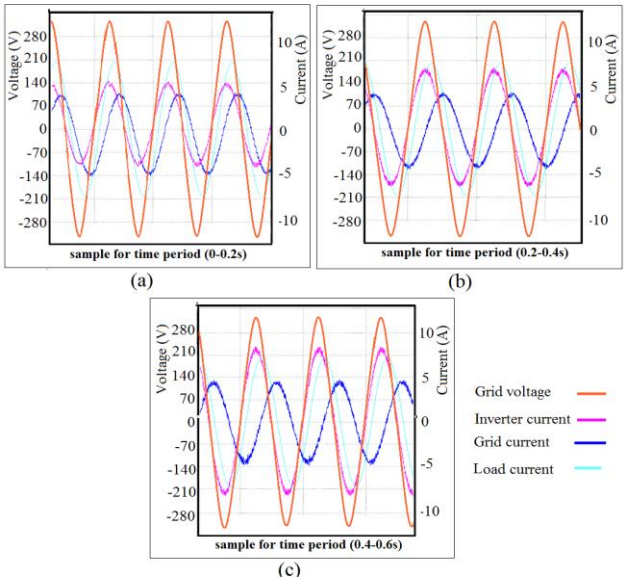

Fig. 12. V_{grid}, I_{inv}, I_{Grid} and I_{Load} with constant load and insolation variations a) Insolation= 0.4kW/m^2, b) Insolation= 0.6k W/m^2, c) Insolation= 0.8 kW/m^2

The THD of the inverter current and the grid current are 1.19%, 1.8% respectively as given in Fig.13.

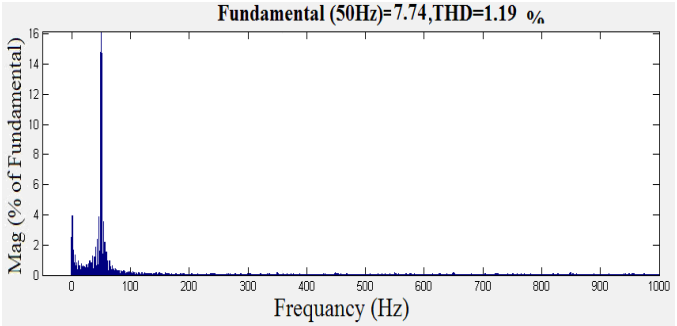

(a) THD and harmonics spectrum of I_{inv}.

ATU-FJIECE, Volume: 3, Issue: 01, Apr, 10, 2024, © 2020 FJIECE, All Rights Reserved

Al-Furat Journal of Innovations in Electronics and Computer Engineering (FJIECE)
ISSN -2708-3985

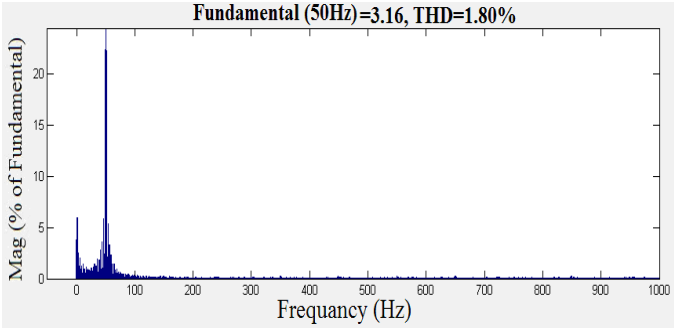

(b) THD and harmonics spectrum I_{Grid}.

Fig.13. THD and harmonics spectrum of I_{inv} and I_{Grid} when constant inductive load and insolation variations

B. Hysteresis Controlled Simulink Model

The Matlab-Simulink model of the Hysteresis current control method is modeled as shown in Fig. 14. The Hysteresis band (h) is selected to be equal to 2A in order to keep the inverter current within the limits, i.e:

$$I_{ref\text{-}up} = I_{ref} + 1 \quad \text{and} \quad I_{ref\text{-}down} = I_{ref} - 1 \qquad (2)$$

The system has been tested with the same two cases with the SPWM method.

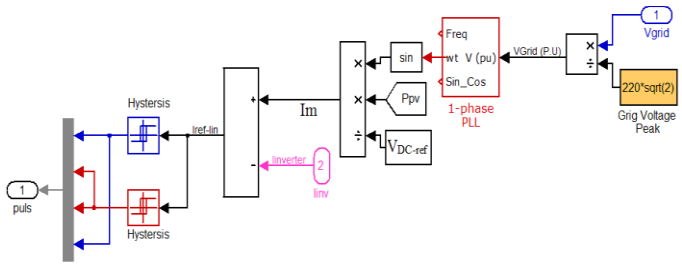

Fig.14. Simulink model of Hysteresis current control method

Case 1: Constant PV arrays power with variable load: Figure 15 shows the waveforms of I_{inv} and I_{ref}, when ($h=2A$). Figure 16 gives the combined waveforms of the I_{inv}, I_{grid} and $I_{load.}$ By comparison with the SPWM control method, the same observations can be seen except for harmonic content. Figure 17 illustrates the THD of the inverter current and current injected to the grid are 4.94% and 6.25 % respectively.

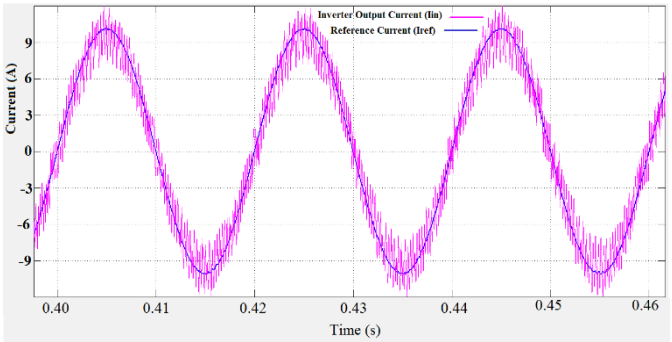

Fig.15. Simulink result of I_{inv} and I_{ref} (h= 2A) during step load changing and constant PV system power

ATU-FJIECE, Volume: 3, Issue: 01, Apr, 10, 2024, © 2020 FJIECE, All Rights Reserved

Al-Furat Journal of Innovations in Electronics and Computer Engineering (FJIECE)
ISSN -2708-3985

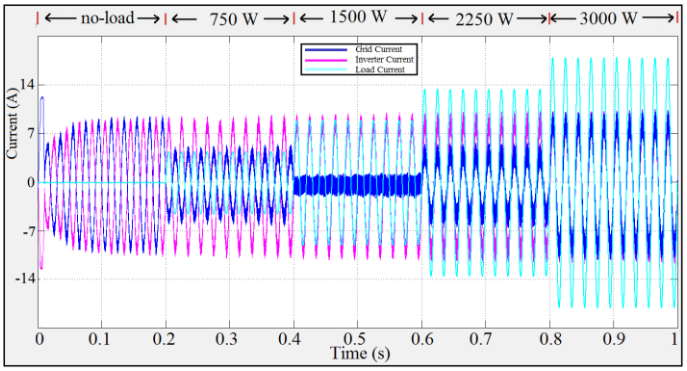

Fig. 16. I_{inv}, I_{Grid} *and* I_{Load} **(h= 2A) during step load changing and constant PV system power**

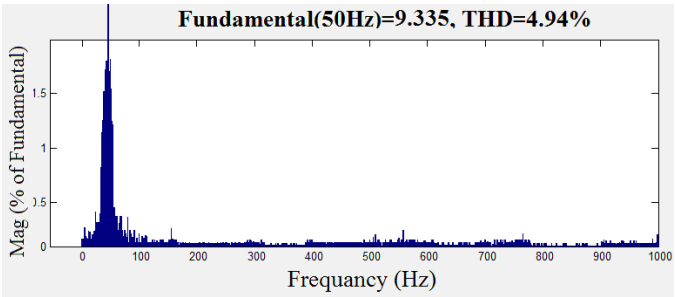

(a) THD and harmonics spectrum of I_{inv}.

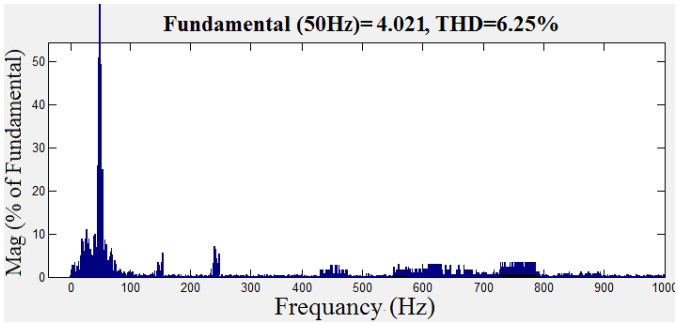

(b) THD and harmonics spectrum I_{Grid}.

Fig. 17. THD and harmonics spectrum of I_{inv} and I_{Grid} when (h=2A) with constant PV power and variable load.

Case 2: Variable PV arrays power with constant inductive load: The Hysteresis controller has been tested in case of the constant inductive load and PV power variations which caused by solar insolation variations that has been given in Fig.10 previously. The waveforms of the I_{inv} and I_{ref} with (h=0.5A) are shown in Fig.20. The THD of the inverter current is 2.77% and the THD of the current injected to the grid is 4.32 % which are given in Fig.21.

ATU-FJIECE, Volume: 3, Issue: 01, Apr, 10, 2024, © 2020 FJIECE, All Rights Reserved

Al-Furat Journal of Innovations in Electronics and Computer Engineering (FJIECE)
ISSN -2708-3985

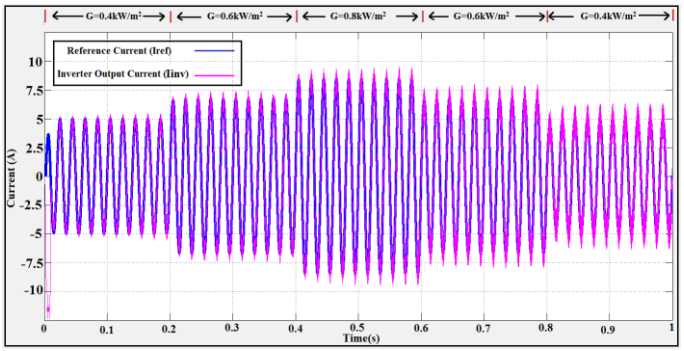

Fig.20. Simulink results of I_{inv} and I_{ref} when hystersis band (h=0.5A) with constant load and variable insolation.

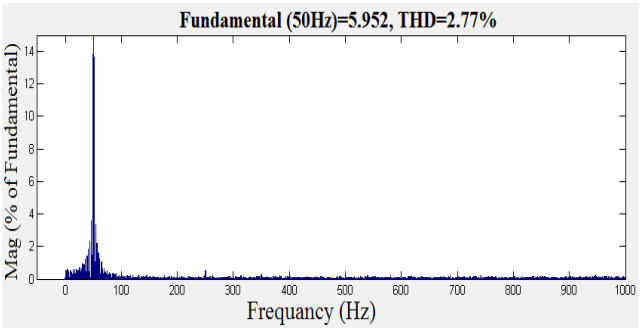

(a) THD and harmonics spectrum of I_{inv}.

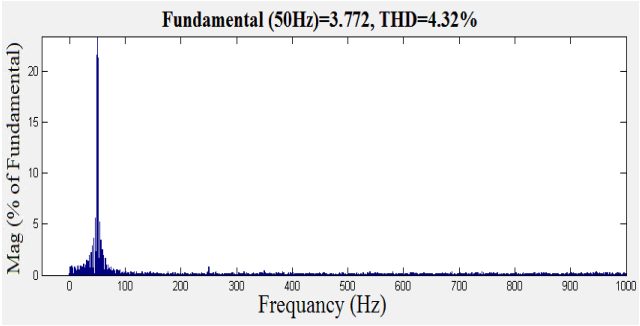

(b) THD and harmonics spectrum I_{Grid}.

Fig.21. THD and harmonics spectrum of I_{inv} and I_{Grid} when (h=0.5A) with constant insolation and variable load

CONCLUSION

This paper designed and simulated 2 kW rated power of two stages single phase grid tied PV inverter. Two CC methods are discussed and simulated. These methods are SPWM and HCC. The two method are tested under different conditions such as load changes and insolation to verify their performance. The simulation results shows that both methods offer approximately identical results for the inverter output current injected to the main grid. The difference can be observed in THD value, where in HCC method has higher than SPWM method. To overcome this limitation, Hysteresis band is reduced, but this would increase the switching frequency and hence increase losses. Therefore, the Hysteresis band is chosen in such way that a tradeoff between low THD and low losses.

ATU-FJIECE, Volume: 3, Issue: 01, Apr, 10, 2024, © 2020 FJIECE, All Rights Reserved

REFERENCES

[1] Ghulam Mujtaba, Zeeshan Rashid, Farhana Umer, Shadi Khan Baloch, G. Amjad Hussain, and Muhammad Usman Haider, "Implementation of Distributed Generation with Solar Plants in a 132kV Grid Station at Layyah Using ETAP", International Journal of Photoenergy, Vol. 2020, June 2020.

[2] Juan Payeras, "Utility-Scale Solar Photovoltaic Power Plants", A Project Developer's Guide, International Finance Corporation 2015, Pennsylvania Avenue, N.W. Washington, 2015.

[3] E. Isen, "Modelling and Simulation of Hysteresis Current Controlled Single-Phase Grid-Connected Inverter", Conference Paper, Amsterdam, Netherlands, Part I, pp. 322-326, August 2015.

[4] P. Rajesh, R. I. Vais, S. Yadav, and P. Swarup, "A Modified PI Control for Grid-tied Inverters to Improve Grid Injected Current Quality", International Journal of Engineering and Technology (IJET), Vol. 9, No. 3S, pp. 529-534, July 2017.

[5] M. Antchev and A. T. Mitovska,"Comparative Analysis of Hysteresis and Fuzzy-Logic Hysteresis Current Control of a Single-Phase Grid-Connected Inverter", American Journal of Electrical Power and Energy Systems, Vol. 4, No. 6-1, pp. 8-12, 2015.

[6] H. Su Bae, J. Hu Park, B. H. Cho and G. J. Yu, "New MPPT Control Strategy for Two-Stage Grid-Connected Photovoltaic Power Conditioning System", Journal of Power Electronics, Vol. 7, No. 2, pp. 174-180, 2007.

[7] D. H. Al_Maamoury, M. Bin Mansor and A. A. Al_Obaidi, "Active Power Control For A Single-Phase Grid-Connected PV System", International Journal of Scientific & Technology Research Vol. 2, Issue 3,pp. 198-202, 2013.

[8] P. K. Hota1, Ba. Panda and Bh. Panda, "A Simple Current Control Strategy for Single-Stage Grid Connected Three-Phase PV Inverter", American Journal of Electrical and Electronic Engineering, Vol. 4, No. 4, pp. 102-109, 2016.

[9] S. D. Patil, S. G. Kadwane, and S. P. Gawande, "Current Control Of Grid Tied Inverter through SHEPWM Method", 1st International Conference on Power Engineering, Computing and CONtrol, PECCON-2017, 2-4 March 2017, VIT University, Chennai Campus, pp. 643–650, Published by Elsevier Ltd. 2017.

[10] A. Chatterjee, K. Mohanty, V. S. Kommukuri, and K. Thakre, "Power quality enhancement of single phase grid tied inverters with model predictive current controller", JOURNAL OF RENEWABLE AND SUSTAINABLE ENERGY 9, 015301, 2017.

[11] Nasir Hussein Selman, Jawad Radhi Mahmood, "Design and Simulation of two Stages Single Phase PV Inverter operating in Standalone Mode without Batteries", International Journal of Engineering Trends and Technology (IJETT), Vol. 37 No. 2, pp.102-109, 2016.

[12] B. Subudhi and R. Pradhan "A Comparative Study on Maximum Power Point Tracking Techniques for Photovoltaic Power Systems", IEEE Transactions on Sustainable Energy, Vol. 4, No. 1, pp.89-98, 2013.

[13] Gulsum Nazl Arpaci, Haluk Gozde and M. Cengiz, "Design and Comparison of Perturb & Observe and Fuzzy Logic Controller in Maximum Power Point Tracking System for PV System by Using MATLAB/Simulink", International Journal of Multidisciplinary Studies and Innovative Technologies, Vol. 3, No. 1, pp. 66-71, 2019.

[14] Linda Hassaine, Mohamed Rida Bengourina, "Control technique for single phase inverter photovoltaic system connected to the grid", Tmrees, EURACA, 4-6 September 2019, Athens, Greece, 2019.

[15] Triet Nguyen-Van, Rikiya Abe and Kenji Tanaka, "A Digital Hysteresis Current Control for Half-Bridge Inverters with Constrained Switching Frequency", Energies 2017, 10, 1601, 2017.

ATU-FJIECE, Volume: 3, Issue: 01, Apr, 10, 2024, © 2020 FJIECE, All Rights Reserved